Nuclear resonance fluorescence in ^{206,207,208}Pb and ^{209}Bi†

D. F. Coope,* L. E. Cannell,‡ and M. K. Brussel
Department of Physics, University of Illinois at Urbana-Champaign, Urbana, Illinois 61801
(Received 2 July 1976)

Using bremsstrahlung produced with 6.6 and 9.7 MeV beams, nuclear resonance fluorescence measurements were made on targets of ^{206,207,208}Pb and ^{209}Bi. Ground state transition widths for previously unknown energy levels with widths $\gtrsim 1$ eV were obtained. An interpretation of several of these levels in terms of a particle-core weak coupling model is suggested.

[NUCLEAR REACTIONS ^{206,207,208}Pb, ^{209}Bi(γ,γ); resonance fluorescence with 9.7 and 6.6 MeV bremsstrahlung. Levels measured E_γ, I_γ at 125° (lab); deduced $g\Gamma_0^2/\Gamma$.]

I. INTRODUCTION

Photonuclear reactions can provide especially valuable information about nuclear structure. The relevant electromagnetic interaction is well understood, amenable to precise calculation, and selective in the nuclear excitations it induces. Only dipole and (less probably) quadrupole transitions can be readily observed below the excitation energy of the giant dipole photonuclear resonance.

This work surveys lead and bismuth energy levels with the photon scattering techniques of nuclear resonance fluorescence (NRF).[1] In our application the photon source was bremsstrahlung produced with electron beams from the University of Illinois accelerator MUSL-1[2] (*microton using a superconducting linear* accelerator). For the first time electron beams from a high duty factor (≃40%) accelerator were used to scan an excitation energy range up through neutron thresholds, previous efforts having been limited either by maximum available beam energies (e.g., the Bartol group[3]), the discreteness of the photon source energy spectrum,[4,5] or the duty factor.[6]

Our experimental arrangement resembles that used by the Bartol group,[3] but our procedure differs in that in any given run we analyze a much larger portion of the scattered spectrum. This is feasible when the transitions are relatively strong and distinct, as they are in the lead region. It has the virtue of allowing a direct intercomparison of transitions. It is less advantageous in measuring weak transitions ($\lesssim$1 eV) due to the nature of the bremsstrahlung background. In that case the increased sensitivity of the Bartol procedure is recommended. That procedure was not appropriate for the broad survey we intended.

It is well known that ^{208}Pb serves as a reference[7] for neighboring nuclei. To know its excitations and those of its neighbors is of great importance in testing shell model calculations, but measurements upon the bound states of these nuclei have until recently been restricted to their first few MeV of excitation. Measurements with particle beams have been limited both by available beam energies and overall energy resolutions. Even with the improved resolution provided by magnetic spectrometers, it has remained difficult to resolve individual levels at high excitations, especially in view of the nonselective character of the hadronic beams used. The advent of the Ge(Li) detector largely obviated these difficulties for studies with photon beams, replacing them with the difficulties of producing suitable photon (or electron) beams.

Early photon studies of nuclei in the lead region of the Periodic Table at energies below their (γ,n) thresholds were made by Reibel and Mann,[8] Fuller and Hayward,[9] and Axel *et al.*[10] Large variations of the elastic scattering cross section with photon energy were observed, being attributed to statistical fluctuations of the ground state transition strength function. The ^{208}Pb data were consistent with the existence of a few strongly excited, widely spaced energy levels having a spin of $J=1$. In neighboring ^{206}Pb and ^{209}Bi the elastic scattering strength seemed to spread over many more levels than in the doubly magic ^{208}Pb, but the total strength over similar regions of observation was about the same.

More recently virtually all of the levels of ^{208}Pb excited strongly by photons (presumably $J=1$ states) have been observed with relatively good energy resolution.[11,12] Shell model configurations for some of these have been extracted from experiments with charged particle reactions.[13-17] Theoretical estimates[18,19] of the electric dipole strength and its energy distribution fairly well-match the excitation strength observed in these experiments. However, information about the near neighbors of ^{208}Pb is scarce. Our present survey is intended to provide such information in the excitation region extending up to neutron separation energies.

After giving some basic experimental formulas in Sec. II and an accounting of experimental procedures in Sec. III, we discuss our results in Sec. IV, presenting energies and excitation strengths of observed levels in terms of a weak coupling of valence nucleons to a ^{208}Pb core.

II. BASIC RELATIONS

By NRF[1] we mean the photoexcitation from the ground state of a nucleus to some excited state at energy E and the subsequent deexcitation by photon emission either to the ground state or to some other (excited) state i. If Γ_i represents the partial decay width of the initially excited state through photon channel i, and Γ is the total decay width for all processes, then the cross section for resonance fluorescence by γ rays of wavelength $2\pi\lambda\!\!\!^{-}$ is given by

$$\sigma_{sc}^{i}(E)=\pi\lambda\!\!\!^{-2}\,\frac{2J_e+1}{2(2J_0+1)}\,\frac{\Gamma_0\Gamma_i}{(E-E_r)^2+\frac{1}{4}\Gamma^2}\,. \tag{1}$$

Γ_0 is the energy width corresponding to photon decay from the initially excited state to the ground state. J_e (J_0) is the spin of the initially excited (ground) state. If only photon decay channels are significantly open, the total absorption cross section is given by

$$\sigma_{\rm abs}(E)=\sum_i \sigma_{sc}^{i}(E)=\frac{\Gamma}{\Gamma_0}\,\sigma_{sc}^{0}(E)\,. \tag{2}$$

Expressions (1) and (2) predict large peak absorption cross sections which are not realized in experimental measurements due to the thermal motions of the nuclei in the target (Doppler broadening).

If the number of incident photons per unit energy as a function of energy E is represented by $N(E)$, then the number of photons scattered into channel i by a target of thickness N_s nuclei/(unit area) is given by

$$N(E)\mathcal{G}'=N(E)\int_{\rm resonance} dE\,\{1-\exp[\alpha N_s\sigma_{\rm abs}(E)-N_s\sigma_{\rm at}(E)]\}[\sigma_{sc}^{i}/(\sigma_{\rm abs}+\sigma_{\rm at}/\alpha)]\,. \tag{3}$$

[$N(E)$, evaluated at the resonance energy, is assumed to be constant over the resonance and has been factored from the integral.] α represents the relative abundance in the sample of the particular nucleus in question. $\sigma_{\rm at}$ represents the total atomic photon cross section at the energy E. The integral $\mathcal{G}'$, which is closely related to one well known in neutron resonance work,[20] can be evaluated analytically only under certain conditions and/or approximations. In general, and for our purpose, it was evaluated numerically using the Doppler broadened cross sections and the assumed values of the nuclear parameters of Eqs. (1) and (2).

N_d, the number of elastically scattered ($i\equiv 0$) photons associated with a nuclear level at excitation energy E_r, detected in a particular escape peak of the detector, is given by the expression

$$N_d=N(E_r)\epsilon(E_r)\mathcal{G}'W(\theta)\,, \tag{4}$$

$\epsilon(E_r)$ is the detection efficiency for the escape peak and includes absorptive and geometrical effects. $W(\theta)$ is an angular distribution factor.

In order to find the experimental value of $\mathcal{G}'$ and hence the nuclear energy level width parameters, the product $N(E_r)\epsilon(E_r)$ must be determined. The method used is described in Sec. III.

The integral $\mathcal{G}'$ for our measurements tends to determine the value of the parameter combination $g\Gamma_0^2/\Gamma$ [$g\equiv(2J_e+1)/(2J_0+1)$]. Under favorable conditions self-absorption experiments or scattering experiments using a range of target thicknesses can be used to determine Γ_0 and Γ_0/Γ separately for a given value of g. Similarly in favorable conditions, an angular distribution measurement can determine the statistical factor g, and a polarization measurement can determine the parity change associated with a transition.

III. EXPERIMENTAL PROCEDURES

A. Apparatus

The bremsstrahlung used was produced from electron beams coming from MUSL-1.[2] 6.6 and 9.7 (±0.2) MeV beam energies were used almost exclusively. Average currents of 5 μA (12.5 μA during the macroscopic pulse) at 9.7 MeV and 7 μA at 6.6 MeV, with macroscopic duty factors of 40%, were available at a bremsstrahlung converter. The experimental setup is shown in Fig. 1. An essentially parallel beam of diameter less than 5 mm entered the experimental area. It was defined vertically and horizontally by nonintercepting slits before entering a doubly focusing 70° bending magnet. This beam was positioned on a 100 mg/cm^2 gold foil bremsstrahlung target by passing it through a 4 mm diam hole in a quartz viewscreen immediately preceding the gold foil. The quartz screen could be viewed with a television monitor throughout the course of a run to detect any movement of the beam on the converter. The beam was stopped in a 15 g/cm^2 thick block of carbon inside a Faraday cup. The bremsstrahlung intensity was

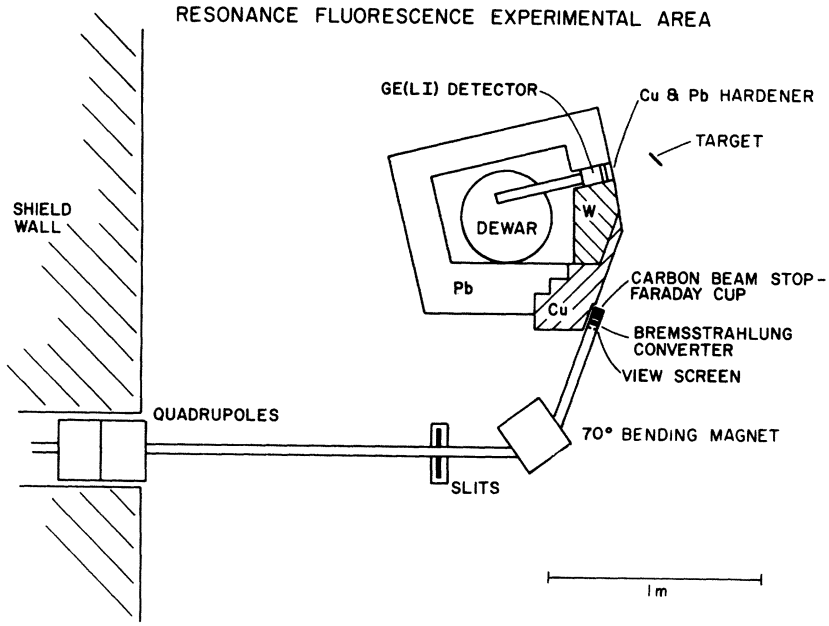

FIG. 1. The experimental area. The electron beam from the accelerator enters at the left and is focused through a view screen placed just before the bremsstrahlung converter. The carbon beam stop is part of a Faraday cup used to monitor the bremsstrahlung intensity.

monitored by the Faraday cup electron current.

The bremsstrahlung beam so produced was intercepted by a square target sample, 10 cm on a side, located about 80 cm from the source. The thicknesses and isotopic abundances of the five targets studied in this experiment are given in Table I. Scattered photons were detected by a 50 cm^3 Ge(Li) detector placed at 125° with respect to the beam direction, an angle favorable for dipole scattering but unfavorable for atomic scattering. Figure 1 shows that tungsten and copper were used to shield the Ge(Li) detector from bremsstrahlung emanating from the converter. The copper [(γ,n) threshold at 10 MeV] served to reduce neutron production in the tungsten [(γ,n) threshold at 7.8 MeV] by attenuating the bremsstrahlung significantly before it could interact in the tungsten. This greatly reduced the high energy ($\gtrsim$3 MeV) γ background produced by (n,γ) processes in the experimental area, and helped to protect the detector from neutron damage. Between the Ge(Li) detector and the target was an absorber combination of copper (7 cm) and lead (1.25 cm), chosen to emphasize the higher energy part of the scattered spectrum.[21] The target-in target-out ratio of the counting rate for photon energies greater than a few MeV was then typically 20:1 for a 3.6 g/cm^2 lead target.

Although the instantaneous counting rate from the Ge(Li) detector was typically 30 000 counts/sec, in the energy region of interest it was often less than a thousand counts/sec. The effects of pileup were minimized through the use of a gated integrator.[22] At a counting rate of 30 000 counts/sec the energy resolution obtained in the Ge(Li) for 8 MeV photons was typically 8 keV full width at half maximum. The pileup losses (which were accounted for) were always less than 8%. The signals, sorted by pulse height in a 1024 channel analog-to-digital converter, were processed on line in a PDP-15 computer. A stable, precision pulser which simulated two energies in the pulse height

TABLE I. Target characteristics.

Target	Isotope	Abundance	Thickness ($g$cm^{-2})	$-Q(\gamma,n)$ (MeV)
^{206}Pb	206	88%	2.43	8.1
	207	9%		6.7
	208	3%		7.4
^{207}Pb	206	2.6%	10.4 average[a]	
	207	84.8%		
	208	12.6%		
^{208}Pb	206	25.8%	1.78	
	207	1.7%		
	208	72.5%		
^{208}Pb	206	25.8%	3.30	
	207	1.7%		
	208	72.5%		
Bi	209	100%	3.11	7.5

[a]Open right circular cylinder: 5.4 cm outer diameter ×4.7 cm inner diameter × 5.5 cm. Mass = 309 g.

TABLE II. Level widths used to calibrate photon flux.

Energy (keV)	Nucleus	Γ_0 (eV)	Reference
8920	^{11}B	4.5 ± 0.5	26
8209	^{31}P	1.4 ± 0.1	27
7332	^{208}Pb	52 ± 6	24
7139	^{31}P	1.52 ± 0.15	27
7083	^{208}Pb	10.6 ± 1.3	24
		17 ± 2	5
7063	^{208}Pb	20.2 ± 2.5	24
		31 ± 3	5
6721	^{208}Pb	16.1 ± 1.6	24
6333	^{88}Sr	4.5 ± 0.6	25
6212	^{88}Sr	3.0 ± 0.4	25
5513	^{208}Pb	25.5 ± 3.4	24
5293	^{208}Pb	8.4 ± 1.4	24
5021	^{11}B	1.73 ± 0.14	26
4842	^{208}Pb	8.2 ± 1.4	24
		5.1 ± 0.8	12
4085	^{208}Pb	0.5 ± 0.1	12

spectrum (at the low and high ends) was used to monitor and correct the energy spectrum for zero and gain shifts as it was being accumulated.

B. Flux calibration

The product of the photon flux and the detector efficiency, $N(E)\epsilon(E)$, was measured in this experiment by observing nuclear levels with known cross sections and solving Eq. (4) for $N(E)\epsilon(E)$. In the energy range above 4.0 MeV few accurately measured level widths could be found in the literature. For this reason we used the University of Illinois tagged photon facility[23] to determine cross sections for those strong levels whose nearest neighbors were presumed not to lie within the tagged photon energy resolution. Since the energy levels in ^{208}Pb have large widths and are widely spaced between 4.8 and 7.4 MeV, such average cross section measurements can be used to determine their level widths. The results of such determinations for ^{208}Pb[24] and ^{88}Sr[25] as well as data from the literature[12,5,26,27] are given in Table II. The listed values of Γ_0 were used to calculate values of $N(E)\epsilon(E)$ for both our 6.6 and 9.7 MeV bremsstrahlung beams. The detector efficiency[28] and the effect of the absorber were then removed from $N(E)\epsilon(E)$ and the photon flux was expressed as a function of the energy interval $E' \equiv E_{\text{endpoint}} - E$: $N(E') \equiv N(E_{\text{endpoint}} - E)$. For simplicity only, and consistent with the precision of the results, these points were fitted by an exponential function of E', as shown in Fig. 2. This curve for $N(E')$ was then used to calculate the decay widths. Fortunately, only three small transitions in ^{208}Pb at 6.357, 6.305, and 6.262 MeV are affected by the poor fit in Fig. 2 below $E' = 0.7$ MeV.

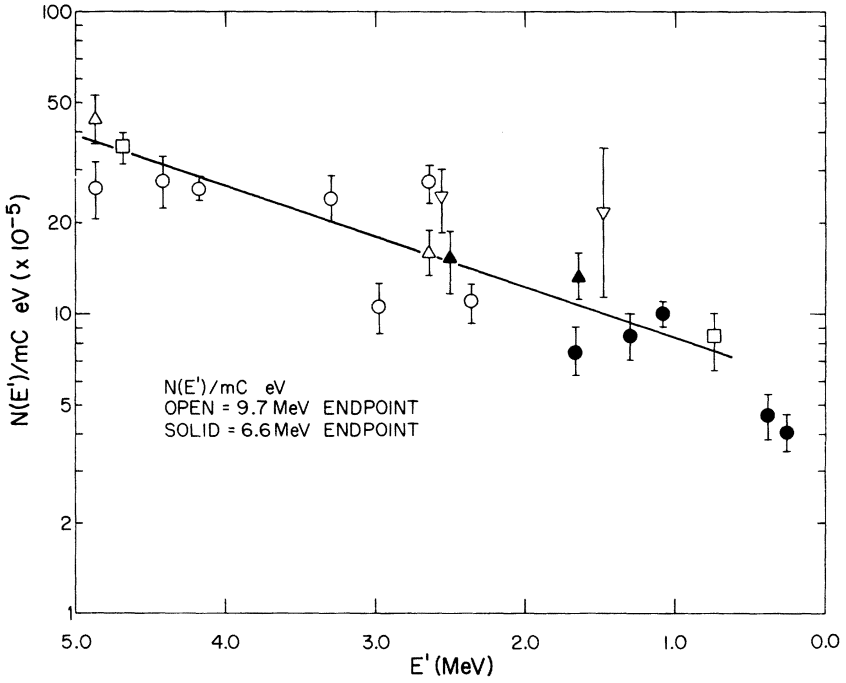

FIG. 2. The photon flux (per mC eV) versus $E' \equiv E_{\text{endpoint}} - E$. Solid (open) symbols refer to measurements made with 6.6 (9.7) MeV electron beams. The error bars indicate uncertainties in the assumed values of $g\Gamma_0^2/\Gamma$ (see Table II).

TABLE III. The estimated smallest values of $g\Gamma_0^2/\Gamma$ that could have been determined for isolated levels at 5.5 and 7 MeV in this experiment.

Isotope	$g\Gamma_0^2/\Gamma$ (eV) 5.5 MeV	7.0 MeV
^{206}Pb	0.5	4
^{207}Pb	3	...
^{208}Pb	1	8
^{209}Bi	1	4

C. Peak identification sensitivity

Table III shows the approximate value of $g\Gamma_0^2/\Gamma$ for the smallest peak that could have been discerned at two excitation energies, 5.5 and 7 MeV, for each isotope we have studied. The quoted sensitivity is specific to the length of our runs, the size of our targets, and our experimental arrangement.

IV. RESULTS AND DISCUSSION

The energies of those peaks that were clearly observed in our spectra are listed with their strengths in Table IV. Since ^{208}Pb (12.5%) was present in our ^{207}Pb target, some ^{207}Pb levels may have been missed if they occurred at energies corresponding to ^{208}Pb levels. For example, the level at 5.513 MeV in Fig. 4 is statistically consistent with an assignment of ^{208}Pb. For all the transitions listed in Table IV we have assumed a dipole character and $\Gamma_0/\Gamma = 1$. Thus, $g\Gamma_0/\Gamma = 3$ for ^{206}Pb and ^{208}Pb; for ^{207}Pb and ^{209}Bi, we assume that $g\Gamma_0/\Gamma = 1$. Except for the level at 6.753 MeV in ^{207}Pb, for which an 8 MeV beam was used, all the peaks listed were observed using either 6.6 or 9.7 MeV electron beams. Criteria used for the identification of peaks were (1) that the full energy, first, and second escape peaks be visible, and (2) that the relative number of counts in each escape peak be appropriate for the yield of the associated full energy peak. The energies listed in Table IV are accurate to ±3 keV for ^{208}Pb and ±5 keV for the other isotopes. Percentage uncertainties in values of $g\Gamma_0^2/\Gamma$ are also listed, having been estimated from the counting statistics and the uncertainty in our knowledge of $N(E)\epsilon(E)$.

^{208}Pb

Spectra for 6.6 and 9.7 MeV bremsstrahlung scattering from an enriched ^{208}Pb target are shown in Fig. 3. Prominent peaks are seen below the neutron threshold (7.37 MeV) at 7.332, 7.083, 7.063, 6.721, 5.513, 5.293, and 4.842 MeV. The level at 4.842 MeV has been reported in a photon scattering experiment by Swann[29] to be $J^\pi = 1^+$, but more recent work[30] favors instead $J = 1^-$. Lindgren *et al.*[31] have reported $M1$ strength at ~6.2 MeV from 180° inelastic electron scattering data, probably corresponding to one or more of the small levels seen in our measurements in that energy region. We obtain a value of $g\Gamma_0^2/\Gamma$ of 12± 5.5 eV for the largest of these at 6.262 MeV. Peaks at 5.902 and 5.039 MeV are caused by scattering from ^{206}Pb in the sample.

Except for the three peaks near 6.3 MeV, all of these levels in ^{208}Pb have been previously observed. Charged particle scattering[13,14] and transfer reaction[15-17] experiments have been used to determine the neutron particle-hole (p-h) configuration strengths of some of these excitations. These experiments have indicated that:

(1) The 5.293 MeV state contains almost all of the $|s_{1/2}p_{1/2}^{-1}\rangle$ neutron configuration strength not included in the giant dipole resonance (GDR).
(2) The 5.513 MeV state is mixed in its neutron p-h character.[15]
(3) Most of the $|d_{3/2}p_{1/2}^{-1}\rangle$ neutron configuration strength is located at 5.94 MeV[15,17] and has the assignment $J^\pi = 1^-$[14]; it has been seen neither in our measurements nor in those of Knowles *et al.*[11]
(4) The states observed in photon scattering experiments[11] at 6.721, 7.063, 7.083, and 7.332 MeV do not contain significant admixtures of the $|s_{1/2}p_{1/2}^{-1}\rangle$, $|d_{3/2}p_{1/2}^{-1}\rangle$, or $|d_{5/2}p_{1/2}^{-1}\rangle$ neutron configurations.[14,15,17] This concentration of (presumably $E1$) photon excitation strength near 7 MeV in ^{208}Pb might therefore be composed largely of proton 1p-1h configurations in agreement with predictions of Harvey and Khanna.[19]

It is interesting to note that whereas the 5.94 MeV $|d_{3/2},p_{1/2}^{-1}\rangle$ neutron state is not strongly excited in photon transitions, the 5.293 MeV neutron $|s_{1/2},p_{1/2}^{-1}\rangle$ state is appreciably excited. However, the most strongly excited states observed by us appear to have mixed configurations.

Theoretical explanations of the distribution of electric dipole excitation strength in ^{208}Pb have had only qualitative success. A particle-hole calculation by Gillet, Green, and Sanderson[32] using 25 $1\hbar\omega$ single particle states has described well the general nature of the GDR. These calculations predict most of the dipole strength to be pushed up in energy to form the GDR, only a few percent remaining near the unperturbed 1p-1h configuration energies between 5 and 7 MeV. However, the energy of the predicted GDR is centered 2 or 3 MeV lower than the experimental value. Harvey and Khanna[19] have also reproduced the gross features of the experimentally observed electric dipole strength distribution. Their predicted giant dipole

resonance is similarly centered 2 MeV too low in energy, but reproduces the observed collection of low lying strength in two "miniresonances" about 3.5 MeV apart. These two resonances are characterized as highly mixed neutron or proton particle-hole states, no one state having more than 15% of any one configuration. The neutron miniresonance is located at 4.5 MeV, the proton resonance at 7 MeV. A similar calculation by True, Ma, and Pinkston[18] does not predict this degree of configuration mixing.

The predicted energies and transition rates of all the above calculations[18,19] differ enough quantitatively from our measured values so that a detailed comparison would not be meaningful. On the other hand, inferences about the p-h character of the

TABLE IV. Observed levels and their strengths. *The value for* Γ_0 *assumes* $g\Gamma_0/\Gamma = 3$ *for* ^{206}Pb *and* ^{208}Pb, *and* $g\Gamma_0/\Gamma = 1$ *for* ^{207}Pb *and* ^{209}Bi. Values in parentheses have uncertainties in excess of 50%. Statistical uncertainties are given for well-defined peaks. Total uncertainties include uncertainties in flux calibration. Energy values are believed to be accurate to ±3 keV for the starred (★) ^{208}Pb levels and to ±5 keV for the other levels.

Energy (MeV)	Nucleus	Γ_0 (eV)	Uncertainty (%) Statistical	Total	Other measurements $g\Gamma_0^2/\Gamma$ (eV)	Γ_0 (eV)	References
6.84	(Pb) 206	7.4		40			
6.73		5.5		40			
5.902		4.4	15	40			
5.854		(3.0)					
5.798		(1.0)					
5.689		(0.5)					
5.615		(1.0)					
5.577		(0.5)					
5.039		1.6	15	40			
4.974		0.8		40			
6.753	(Pb) 207	(<10)					
5.716		(3)					
5.600		(8)					
5.490		(12)					
5.223		(8)					
5.209		(8)					
4.980		(7)			4.0 $\Gamma_0/\Gamma = 1$		12
4.875		(13)			3.6 $\Gamma_0/\Gamma = 1$		12
4.847							12
7.332★	(Pb) 208	38	10	35		35,41	11,10
7.083★		14	10	35		15,17 ± 2	11,5
7.063★		29	10	35		15,31 ± 3	11,5
6.721★		15	20	40		15,14	11,10
6.357		(0.5)					
6.305		(1.0)					
6.262		4.1		45			
5.513★		28	2	35		15	11
5.293★		8.6	5	35		5	11
4.842★		6.3	5	35	$J^\pi = 1^+$	5.1 ± 0.8	12
4.085★		0.51		40	$J^\pi = 2^+$	0.5 ± 0.1	12
5.549	(Bi) 209	6.6		40			
5.522							
5.509		17	5	35			
5.498							
5.422		8.3		45			
5.293		12	15	40			
4.845					1.4		12
4.808		(10)			2.7		12
4.771					2.9		12
4.501		(3)					
4.228		(3)					

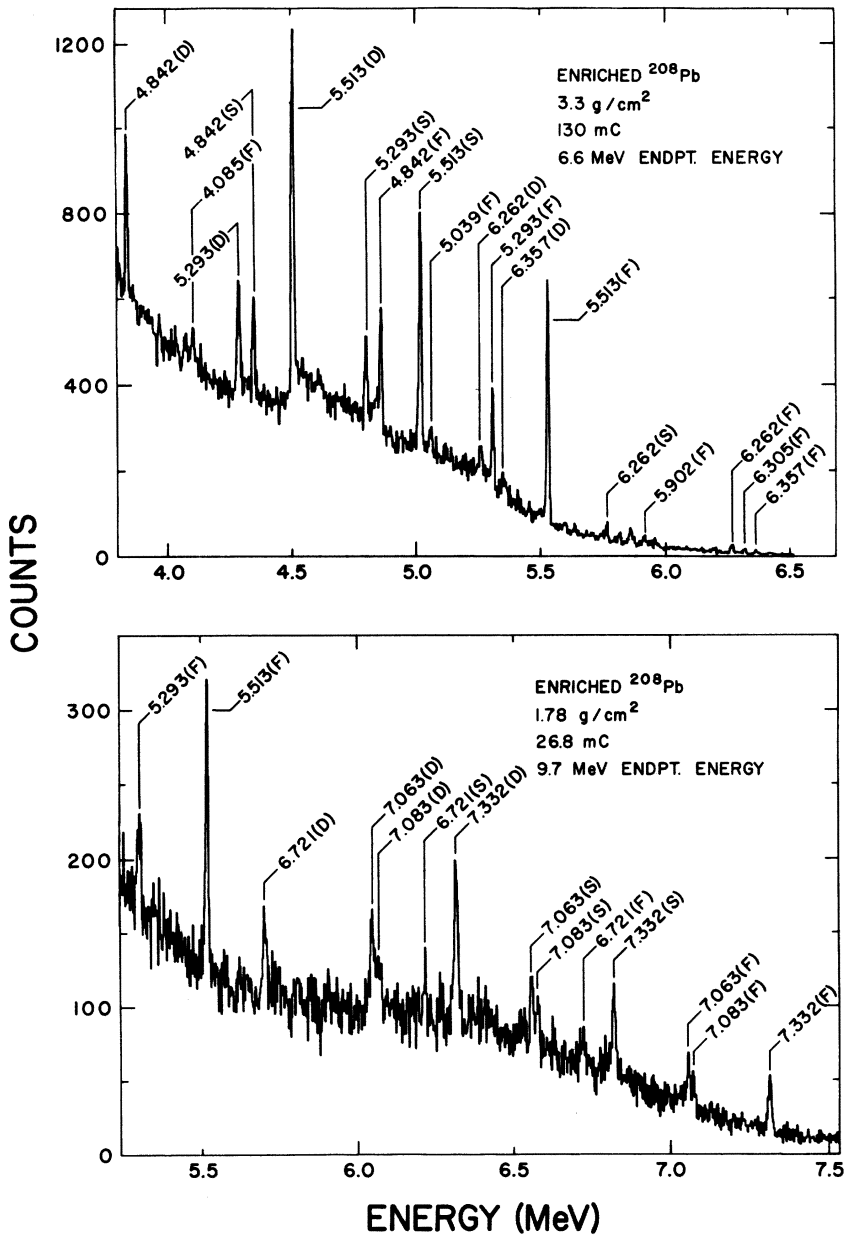

FIG. 3. Spectra for 6.6 MeV (upper figure) and 9.7 MeV (lower figure) bremsstrahlung scattered from enriched ^{208}Pb targets. The values of $g\Gamma_0^2/\Gamma$ for each of the peaks identified are listed in Table IV. F, S, and D refer to the full energy, single, and double escape peaks, respectively. (a) (upper figure) The sensitivity of these measurements may be inferred from the sizes of the peaks at 6.305 and 4.085 MeV which have values of $g\Gamma_0^2/\Gamma$ of approximately 3 and 1.5 eV, respectively. The peaks at 5.902 and 5.039 MeV are from ^{206}Pb in the target. (b) (lower figure) The peak in this spectrum at 5.293 MeV has $g\Gamma_0^2/\Gamma = 26$ eV. Most of the events above 7.4 MeV are due to atomic scattering, since the neutron threshold for ^{208}Pb is at 7.4 MeV.

^{208}Pb states can be drawn from our data on ^{207}Pb and ^{209}Bi. In particular, it is tempting to apply the particle-core–weak-coupling model[33] to these nuclei, since it can explain the presence of multiplet levels at about the same excitation energies as the strongly excited levels in ^{208}Pb.

^{207}Pb, ^{209}Bi

Figure 4 displays spectra for 6.6 MeV bremsstrahlung scattered from samples of ^{207}Pb and bismuth. Although these spectra seem complex, obvious levels appear near 4.842, 5.293, and 5.513

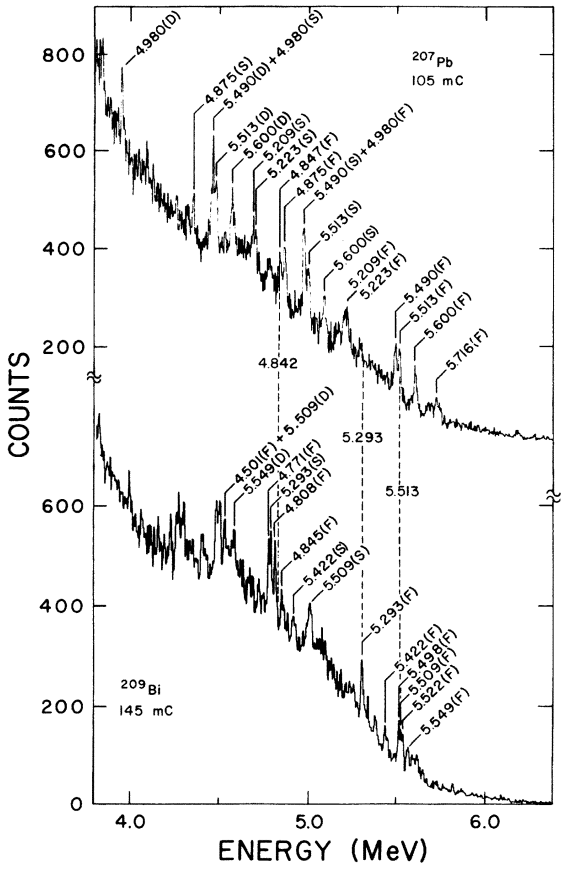

FIG. 4. The spectra for 6.6 MeV bremsstrahlung scattered from a ^{207}Pb target (upper) and a ^{209}Bi target (lower). Not all single escape peaks (labeled S) and/or double escape peaks (D) are indicated. *F* refers to the full energy peak. The dashed lines at 4.842, 5.293, and 5.513 MeV indicate energies where the large levels are observed in ^{208}Pb. The ^{207}Pb target contains 12.6% ^{208}Pb. The peak in the ^{207}Pb target spectrum at 5.513 MeV is probably due to this ^{208}Pb contaminant.

MeV in ^{209}Bi and near 4.842 and 5.513 MeV in ^{207}Pb, precisely the energies of the ^{208}Pb core states. A weak-coupling model would predict a triplet of levels in ^{209}Bi($h_{9/2} \oplus 1^- \rightarrow \frac{7}{2}^+, \frac{9}{2}^+, \frac{11}{2}^+$) and a doublet in ^{207}Pb($p_{1/2} \oplus 1^- \rightarrow \frac{1}{2}^+, \frac{3}{2}^+$) for each $\Delta J^\pi = 1^-$ core excitation. Just what the magnitude of the energy splittings in these multiplets should be depends upon the nature of the particle-core coupling. However, each multiplet seen does seem to have its center of strength near the appropriate ^{208}Pb core energy. The weak-coupling model prediction that the amount of strength ($g\Gamma_0$) in the multiplet should equal the strength in the core state is difficult for us to check since what we determine is $g\Gamma_0^2/\Gamma$, and the branching ratios (Γ_0/Γ) are not known. Table IV shows that the strength we observe in a particular multiplet of ^{207}Pb or ^{209}Bi is not inconsistent with the strength associated with the core excitation.

We emphasize that our assignment of peaks (Fig. 4) to a particular multiplet related to the lead core is more suggestive than definitive. Numerous peaks exist in each of these spectra. Without a firm knowledge of their spins and parities it is risky to infer their parentages. However, weak coupling has been much invoked for lower lying states. In addition to its success in connection with the particle-octupole vibration at 2.614 MeV in ^{208}Pb, Bertrand and Lewis[34] have observed that it persists up to 4.3 MeV in ^{209}Bi, and Swann[12] has suggested weak-coupling levels at 4.1 and 4.8 MeV in ^{207}Pb and ^{209}Bi. Our data would suggest that this model retains validity up to 5.5 MeV. On the other hand, it is natural to expect that as the nuclear ex-

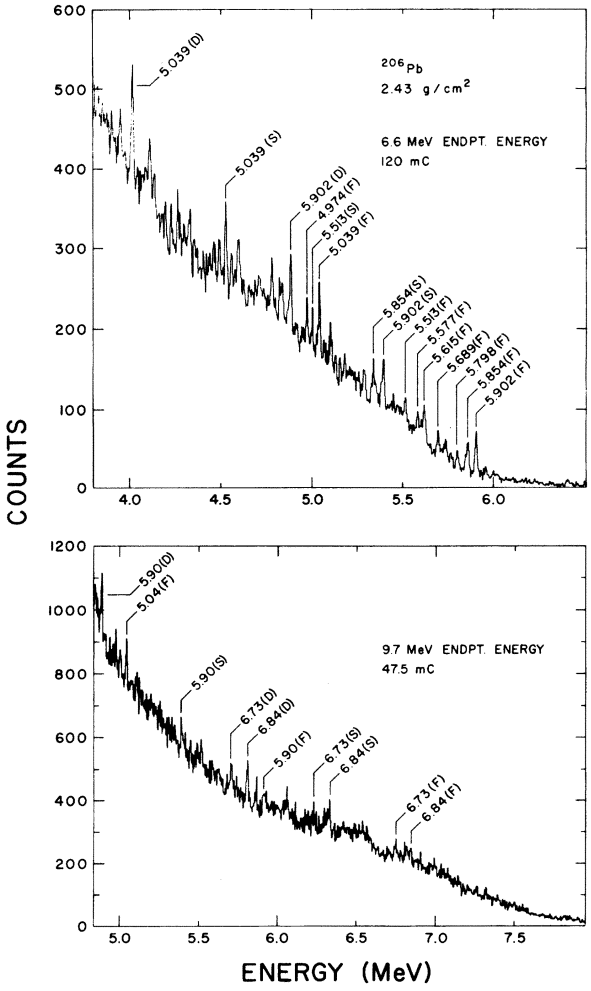

FIG. 5. Spectra for 6.6 and 9.7 MeV bremsstrahlung scattered from a ^{206}Pb target. F, S, and D refer to the full energy, single, and double escape peaks, but not all such peaks are labeled.

citation energy increases the probability of weak coupling will decrease; the greater density of other excitations of the same spin and parity would be expected to couple to the weak-coupling modes and so perturb their identification. A measurement of the total strength of the supposed multiplets would check this idea.

Notably absent from the ^{207}Pb data is a doublet corresponding to the 5.293 MeV level in ^{208}Pb, which has been characterized as predominantly $|s_{1/2}p_{1/2}^{-1}\rangle$ in its neutron particle-hole composition. This state corresponds to the ^{207}Pb ground state plus an $s_{1/2}$ neutron. In view of the strong pairing interaction between two $p_{1/2}$ neutron particles (or holes), one would not expect weak coupling to apply here. The state corresponding to the $|s_{1/2}p_{1/2}^{-1}\rangle$ hole state in ^{208}Pb has been reported at an energy of 4.63 MeV in ^{207}Pb.[35] The 5.513 and 4.842 MeV states in ^{208}Pb, which have a more mixed character,[35] do exhibit weak coupling to ^{207}Pb.

Above an excitation energy of 6.8 MeV in ^{207}Pb and 6 MeV in ^{209}Bi no well defined peaks appear in our spectra. Above 6.8 MeV in ^{207}Pb, no such peaks are expected in view of the threshold for neutron emission at 6.7 MeV. In ^{209}Bi this threshold is at 7.4 MeV. With our experimental sensitivity (Table III), transitions having $g\Gamma_0^2/\Gamma = 5$ eV ought to have been seen. After looking with considerable care we could adduce no evidence for levels reported by Swann[5] near 7.2 MeV in both ^{207}Pb and ^{209}Bi having $g\Gamma_0^2/\Gamma \simeq 20$ eV. That no peaks were seen in ^{209}Bi above 6 MeV might have been the result of competing inelastic transitions, for example to the first excited state of ^{209}Bi at 897 keV ($J^\pi = \frac{7}{2}^-$), but we did not observe such branching. Even a large level, one with $g\Gamma_0 = 20$ eV, might in this instance have a value of $g\Gamma_0^2/\Gamma$ well below 20 eV. Recent data of Laszewski[24] show that a concentration of photon elastic scattering strength equal to about 180 eV does exist between 6.4 and 7.4 MeV in ^{209}Bi. We infer that in ^{209}Bi the corresponding ^{208}Pb strength is shared among a large number of levels which we could not distinguish from the background.

^{206}Pb

We have observed ten previously unreported levels of ^{206}Pb (Table IV). Concentrations of levels at 5.0, 5.5, 5.8, and 6.8 MeV are seen in Fig. 5. It is apparent that the decreasing level spacing in ^{206}Pb above 6 MeV makes individual transitions difficult to discern. The elastic scattering cross section data of Laszewski[24] show a large bump at 7.9 MeV in ^{206}Pb, while we did not distinguish any peaks there. These combined data indicate that the average level spacing corresponding to $E1$ excitations at 8 MeV is less than 20 keV.

Summary

The energies and, in many cases, the ground state decay widths of newly identified states have been determined by photon scattering from ^{206}Pb, ^{207}Pb, ^{208}Pb, and ^{209}Bi. The widths of previously observed large levels in ^{208}Pb were all determined, some for the first time. The absence of detectable levels at energies greater than 6.8 MeV in ^{207}Pb and 6 MeV in ^{209}Bi is noted. Some levels in ^{207}Pb and ^{209}Bi appear highly correlated in energy with states of the ^{208}Pb core and suggest a weak-coupling picture. A quantitative explanation of these levels awaits additional theoretical and experimental efforts, which would appear especially warranted in view of the similarities between the photon scattering spectra for these nuclei and for the ^{208}Pb core.

We are very grateful to Professor P. Axel for his helpful suggestions concerning the data.

---

†This research was supported by the National Science Foundation.

*Present address: Department of Physics and Astronomy, University of Kentucky, Lexington, Kentucky 40506.

‡Present address: Department of Physics, Illinois Benedictine College, Lisle, Illinois 60532.

[1]F. R. Metzger, *Progress in Nuclear Physics* (Pergamon, Elmsford, N.Y., 1959), Vol. 7.

[2]P. Axel, A. O. Hanson, J. R. Harlan, R. A. Hoffswell, D. Jamnik, D. C. Sutton, and L. M. Young, IEEE Trans. Nucl. Sci. NS-22, 1176 (1975).

[3]F. R. Metzger, Phys. Rev. 187, 1680 (1969).

[4]R. Moreh and A. Wolf, Phys. Rev. 178, 1961 (1969).

[5]C. P. Swann, Nucl. Phys. A201, 534 (1973).

[6]N. Shikazono and Y. Kawarasaki, Nucl. Instrum. Methods 92, 349 (1971).

[7]D. A. Bromley and J. Weneser, Comments Nucl. Part. Phys. II, 151 (1968).

[8]K. Reibel and A. K. Mann, Phys. Rev. 118, 701 (1960).

[9]E. G. Fuller and E. Hayward, Nucl. Phys. 33, 431 (1962).

[10]P. Axel, K. Min, N. Stein, and D. C. Sutton, Phys. Rev. Lett. 10, 299 (1963).

[11]A. M. Khan and J. W. Knowles, Bull. Am. Phys. Soc. 12, 538 (1967); J. W. Knowles, A. M. Khan, and W. F. Mills (unpublished).

[12]C. P. Swann, *Proceedings of the International Conference on Photonuclear Reactions and Applications*, (U.S. Atomic Energy Commission Office of Information Services, Oak Ridge, Tennessee, 1975), p. 317.

[13]C. F. Moore, J. G. Kulleck, P. von Brentano, and

F. Rickey, Phys. Rev. 164, 1559 (1967).
[14]J. G. Cramer, P. von Brentano, G. W. Phillips, H. Ejiri, S. M. Fergusen, and W. J. Braithwaite, Phys. Rev. Lett. 21, 297 (1968).
[15]E. D. Earle, A. J. Ferguson, G. Van Middelkoop, and G. A. Bartholomew, Phys. Lett. 32B, 471 (1970).
[16]R. Ballini, N. Cindro, J. Delaunay, J. P. Fouan, O. Nathan, and J. P. Passerieux, Phys. Lett. 26B, 215 (1968).
[17]M. Dost and W. R. Hering, Phys. Lett. 26B, 443 (1968).
[18]W. W. True, C. W. Ma, and W. T. Pinkston, Phys. Rev. C 3, 2421 (1971).
[19]M. Harvey and F. C. Khanna, Nucl. Phys. A221, 77 (1974).
[20]J. Rainwater, in *Encyclopedia of Physics*, Nuclear Reactions I, edited by S. Flügge (Springer-Verlag, Berlin, 1957), Vol. XL, p. 373.
[21]D. F. Coope, Ph.D. dissertation, University of Illinois, 1975 (unpublished).
[22]V. K. Rasmussen, Nucl. Instrum. Methods 83, 39 (1970).
[23]J. S. O'Connell, P. A. Tipler, and P. Axel, Phys. Rev. 126, 228 (1962); P. A. Tipler, P. Axel, N. Stein, and D. C. Sutton, *ibid.* 129, 2096 (1963).
[24]R. M. Laszewski, Ph.D. dissertation, University of Illinois, 1975 (unpublished).
[25]L. E. Cannell, D. F. Coope, R. M. Laszewski, and M. K. Brussel, Bull. Am. Phys. Soc. 19, 999 (1974); L. E. Cannell, Ph.D. dissertation, University of Illinois, 1976 (unpublished).
[26]F. Ajzenberg-Selove and T. Lauritsen, Nucl. Phys. A114, 20 (1968); F. Ajzenberg-Selove, *ibid.* A248, 1 (1975).
[27]P. M. Endt and C. van der Leun, Nucl. Phys. A214, 257 (1973).
[28]F. C. Young, A. S. Figuera, and G. Pfeufer, Nucl. Instrum. Methods 92, 71 (1971).
[29]C. P. Swann, Phys. Rev. Lett. 32, 1449 (1974).
[30]R. M. Del Vecchio, S. J. Freedman, G. T. Garvey, and M. A. Oothoudt, Phys. Rev. C 13, 2089 (1976); L. W. Fagg (private communication).
[31]R. A. Lindgren, W. L. Bendel, L. W. Fagg, E. C. Jones, J. W. Lightbody, and S. P. Fivozinsky, Bull. Am. Phys. Soc. 20, 629 (1975).
[32]V. Gillet, A. M. Green, and E. A. Sanderson, Nucl. Phys. 88, 321 (1966).
[33]A. de-Shalit, Phys. Rev. 122, 1530 (1961).
[34]F. E. Bertrand and M. B. Lewis, Nucl. Phys. A168, 259 (1971).
[35]P. A. Dickey, J. G. Cramer, and D. Chiang, University of Washington Annual Report of Nuclear Physics Laboratory, 1976 (unpublished), p. 75.